Improve CAVs Safety by Proper Vehicle Longitudinal Speed Planning with the Preview of Path Friction and Curvature*

Liming Gao, Craig Beal, Kshitij Jerath, Daniel Fescenmyer, *Sean Brennan.* IEEE Member

***Abstract*— The improvement in vehicle safety can be achieved by limiting the vehicle speed based on the road condition. In this paper, we first introduce an idea of road friction preview through CAVs with shared roadway databases. Then we present an algorithm to generate a longitudinal vehicle velocity limit profile based on the desired path curvature and the preview of path friction. Moreover, the preview distance is discussed to ensure the vehicle has sufficient time to take action for upcoming hazardous situations. Finally, the efficiency of work is demonstrated through an application case where a vehicle with a simple driving controller can follow the path well with the preview of velocity.**

I. INTRODUCTION

The traffic accident is fatal and has a huge negative influence on economic costs. [follow some data from reference] Many factors attribute to safety, but a large part of the accidents are caused by slick roads (snow, ice, raining, etc.) and overspeeding. (make it positive: maximize the safety throughout the highway system in any condition)

One way to make cars safer is the development of the ADASs (Advanced Driver Assistance Systems) such as EBS, LKA, and ESC, etc., which can assist the driver to follow the desired path stably in hazardous situations. The assistance system can be categorized into lateral control, longitudinal control, and hybrid control. The controller can output proper steering angle and/or driving/braking torque command once the vehicle is out of stability. For example, Yu, et al. [1] designed a feedback-feedforward steering controller to improve the vehicle stability when hard-braking maneuvers on road with split friction. Li, et al. presented a torque control strategy for the situation of abrupt changes in the road friction [2].

However, most of the controllers are activated only when the vehicle states have a significant deviation from the nominal value. Additionally, the controller has a stable region. Consequently, the controller even fails to keep the vehicle stable if the road condition changes intensively. [ref]

Different from the reaction controller, researchers developed the proactive envelope controller with real-time road friction estimation, which can keep the vehicle within a stable region. But it still can not certainly prevent the vehicle from veering away from the desired path when the road condition changes intensively.

Existing research has shown that appropriate longitudinal velocity planning is vital when following a path with tight curvature change [3]. The idea is to reduce vehicle speed before a potentially dangerous situation is reached, in contrast with widely used stability control systems that only react once loos of control is imminent. The insight is that the vehicle could have a larger stable operating region to follow the desired path with a smaller velocity [4][5].

However, they only consider the variation of curvature for longitudinal planning, and little attention has been paid to the road surface friction condition changing when conducting longitudinal velocity planning. For example, if the vehicle can preview the path friction reduction and slow down appropriately before entering the slick region, then a complicated algorithm is not necessary to stabilize the vehicle. The prior estimation of friction and peak tire force, before the slick region is reached, allows a vehicle chassis control system to work more reliably and proactively [2]. As a result, even a normal steering control algorithm can enable the vehicle to follow the path well.

Unfortunately, it is almost impossible to preview the large area road condition just through the intelligence of individual vehicle, where each vehicle itself constantly measuring and navigating the world using in-vehicle system. A potential solution to preview the road surface friction condition is motivated by the increasing research into the cyber-physical system, especially Connected and Autonomous Vehicles (CAV). This solution takes advantage of network intelligence instead of individual intelligence, where the pre-measured road friction information from the individual vehicle is shared within the network. Within the network, the information can flow between vehicle to vehicle, vehicle to infrastructure, and vehicle to database systems. In this way, each vehicle and roadside unit can measure local road friction [6][7] and share it with the cloud database. Each vehicle in the network can query the aggregated friction information from the shared database. A demo framework of this network is shown in Fig. 1.

*Research supported by NSF.

Liming Gao is a graduate student in Mechanical Engineering at The Pennsylvania State University, University Park, PA 16803, USA (e-mail: lug358@ psu.edu).

Craig Beal is with Department of Mechanical Engineering, Bucknell University, Lewisburg, PA 17837, USA (e-mail: cbeal@bucknell.edu)

Daniel Fescenmyer is a undergraduate student in Mechanical Engineering at The Pennsylvania State University, University Park, PA 16803, USA (e-mail: dzf5248@psu.edu).

Sean Brennan is with the Department of Mechanical Engineering, The Pennsylvania State University, University Park, PA 16803, USA (e-mail: snb10@psu.edu). IEEE Member.

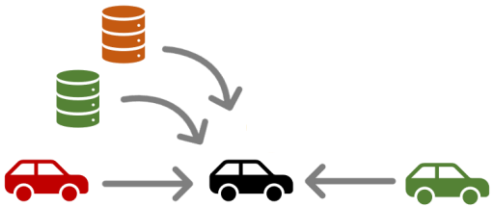

Figure 1. A strategy of road friction preview with a roadside shared roadway database. (need a better diagram to show the data sharing idea) The database can leverage shared intelligence to substantially improve the operation of each individual in the population.

The improvements in vehicle safety can be achieved by limiting the vehicle speed based on the road condition. In this paper, we introduce an idea of road friction preview through database-informed CAV. Then inspired by the work in DDL on vehicle dynamics at the limits of handing [8]–[10], we present an algorithm to generate a longitudinal vehicle velocity limit profile for a given desired path with the preview of path friction. Moreover, relationships are established between data confidence, preview distance, and vehicle speed for a vehicle traversing a roadway system augmented with such a preview system.

The remainder of this paper is organized as follows: Section II discusses the velocity limit profile planning based on the tire limits. Section III analyzes the preview distance. Section IV shows an application case. Finally, a conclusion section summarizes the main results of the work.

II. Vehicle Longitudinal Velocity Planning Given a Reference Path

This section presents the generation of limit speed profile which vehicles can achieve without exceeding available tire friction limits constraints [11]. At first, the longitudinal dynamic driving on the friction circle is derived, and then introduce the approach to describe the path by station s, curvature κ and friction coefficient. Finally, show the detailed velocity planning method.

A. Vehicle Chassis Model and Tire Friction Limits

The vehicle dynamic equations for the planar three states single track model shown in Fig. 2 are:

$$\dot{U}_x = \frac{F_{xf}\cos(\delta) - F_{yf}\sin(\delta) + F_{xr}}{m} + rV_y \tag{1}$$

$$\dot{U}_y = \frac{F_{yf}\cos(\delta) + F_{xf}\sin(\delta) + F_{yr}}{m} - rU_x \tag{2}$$

$$\dot{r} = \frac{a(F_{yf}\cos(\delta) + F_{xf}\sin(\delta)) - bF_{yr}}{I_{zz}} \tag{3}$$

where longitudinal velocity U_x, lateral velocity V_y and yaw rate r are the three states. The vehicle parameters include the vehicle's mass m, yaw moment of inertia I_{zz}, front wheel steering angle δ, and a and b the distance from the vehicle's center of gravity to the front and rear axle respectively. Forces F_{xf}, F_{yf}, F_{xr}, F_{yr} are the forces acting on the front and rear tires.

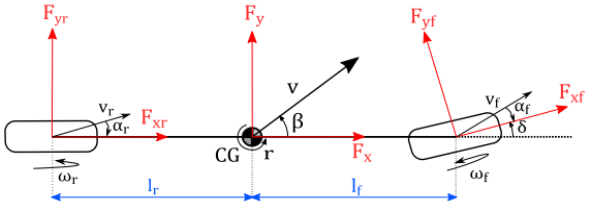

Figure 2. Planar single-tack vehicle chasis model (need update this diagram indicating Ux and Uy, a and b)

The available longitudinal force F_x and lateral force F_y at each tire is constrained by friction circle:

$$F_{xf}^2 + F_{yf}^2 \le \left(\mu F_{zf}\right)^2 \tag{4}$$

$$F_{xr}^2 + F_{yr}^2 \le \left(\mu F_{zr}\right)^2 \tag{5}$$

where μ is the road-tire friction coefficient, and F_{zf} and F_{zr} are the normal force at the front and rear axle respectively. If we ignore the load transfer, the normal forces are $F_{zf} = bmg/(a+b)$, $F_{zr} = amg/(a+b)$.

Determining the limit speed profile requires the vehicle to utilize all the available tire friction to generate forces so that vehicle can operate at acceleration limits to achieve the maximum safe speed [12]. It implies that all tire forces need to remain on the boundary of the friction circle:

$$F_{xf}^2 + F_{yf}^2 = \left(\mu F_{zf}\right)^2 \tag{6}$$

$$F_{xr}^2 + F_{yr}^2 = \left(\mu F_{zr}\right)^2 \tag{7}$$

Fig. 3 shows the tire force when maneuvering through a path left corner. The boundary of the friction circle depends on the road-tire friction coefficient.

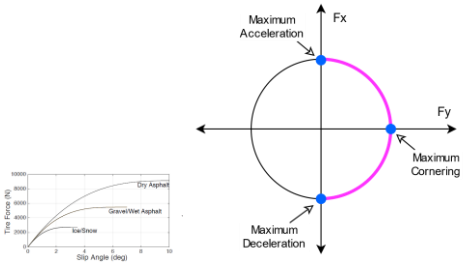

Figure 3. The maximum performance of vehicle can be achieved by driving at the boundary of friction circle.

As we are interested in the longitudinal dynamic, assume the lateral states are steady:

$$\dot{V}_y = 0,\quad V_y = 0,\quad \dot{r} = 0,\quad r = \kappa U_x \tag{8}$$

where κ is the path curvature.

Substituting (6), (7), and (8) into yields:

$$\dot{U}_x = \pm\sqrt{\left(\mu g\right)^2 - \left(\kappa U_x^2\right)^2} \tag{9}$$

Before going further, we add an adjusting parameter λ into the equation (9) for two reasons: a. compensation for the uncertainty of friction preview; b. common driver may not able to operate a vehicle at friction limit as racecar drivers or autonomous driving systems [13]. We have the dynamics equation that depicts the maximum available longitudinal acceleration:

$$\dot{U}_x = \pm\sqrt{\left(\lambda\mu g\right)^2 - \left(\kappa U_x^2\right)^2} \tag{10}$$

where the plus-minus sign (±) corresponds to acceleration and deceleration respectively. The parameters μ and κ in (9) depend on the path position. Thus we introduce the path description method in the following session.

B. Path Representation

This paper doesn't focus on path planning. Therefore, the desired path is assumed to be given. The clothoid path description is widely used for highway road design [14] and vehicle path planning, for example, the racing line [10], [15] and minimum curvature optimal path [16] [17]. A clothoid path can generally be described by a succession of turns - consist of spirals and constant radius arcs - and straight lines. The curvature of the spiral is linearly increasing along with the distance. Thus, the curvature of the whole path can be described by a succession of linear functions.

Without loss of generality, an example path is shown in Fig. 4. The path is given according to the professional racecar driver's racing line, which decomposes the cornering into three phases: an entry clothoid ~~for trail braking~~, a circle arc ~~for pure cornering~~, and an exit clothoid ~~for throttle exit~~ [10]. The curvature and previewed friction coefficient are shown in Fig. 5. The friction can be the minimum friction at each tire for the friction split case. Both of them can be described as a function of the path station: κ(s), μ(s), where the station is the distance traveled along the path.

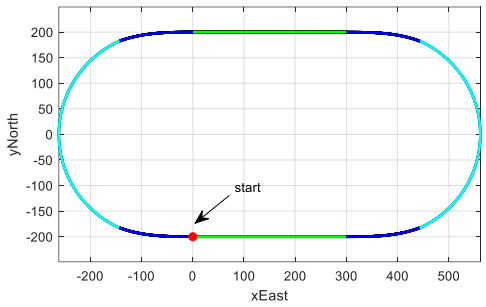

Figure 4. A circular smaple path. (we need to use a better shape: S curve or the PSU test track .

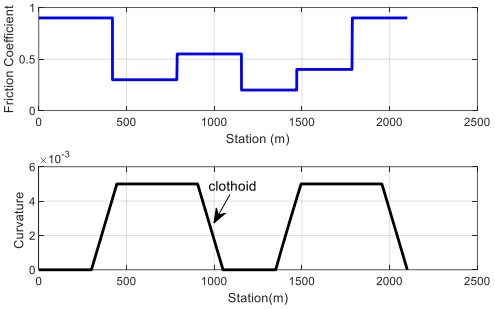

Figure 5. The curvature and previewed friction coefficient for sample path. We assume a abrupt friction changing.

In real-world, the grade of the path also has a significant influence on the vehicle acceleration and deceleration behavior. (I am considering if need to add this term)

C. Velocity Profile Generation

Velocity planning has a significant impact on driving safety, especially when vehicles drive on a road with changing friction and geometry. With the longitudinal dynamic equation (9) and the desired path description, the speed profile can be determined. The approach presented in this paper is inspired by those works: three passes [11], nonlinear optimization [3], segment and iteration [18], where a velocity profile is planned given the path curvature.

Express the longitudinal acceleration with respect to the station:

$$\dot{U}_x = \frac{dU_x}{dt} = \frac{dU_x}{ds}\frac{ds}{dt} = \frac{dU_x}{ds}U_x \tag{11}$$

Substitute (11) into (10) yields:

$$\frac{dU_x(s)}{ds} = \pm\frac{1}{U_x(s)}\sqrt{\left(\lambda\mu(s)g\right)^2 - \left(\kappa(s)U_x^2(s)\right)^2} \tag{12}$$

(12) can be solved using a numerical integration method as we can not find a general analytical solution for all cases.

$$U_x(s_{k+1}) \approx U_x(s_k) \pm \frac{\Delta s}{U_x(s_k)}\sqrt{\left(\lambda\mu(s_k)g\right)^2 + \left(\kappa(s_k)U_x^2(s_k)\right)^2} \tag{13}$$

where $\Delta s = s_{k+1} - s_k$. The solution will be accurate enough if path waypoints are dense, i.e. the Δs is small enough. In this paper, we choose Δs smaller than 0.1m. λ=0.95 is taken.

The first step of generating the speed profile is to find the maximum permissible steady-state vehicle velocity with zero longitudinal acceleration, shown as the "curve limit speed" in Fig. 6. This is given by (14):

$$U_x(s) = \sqrt{\mu(s)g/\kappa(s)} \tag{14}$$

The following next step is a forward integral step:

$$U_x(s_{k+1}) \approx U_x(s_k) + \frac{\Delta s}{U_x(s_k)}\sqrt{\left(\lambda\mu(s_k)g\right)^2 + \left(\kappa(s_k)U_x^2(s_k)\right)^2} \tag{15}$$

It starts from the vehicle's current speed. At each step, the result is compared to the curve limit speed, and the minimum value is taken. This step indicates how fast a vehicle can accelerate.

The final step is a backward integral step:

$$U_x(s_{k+1}) \approx U_x(s_k) + \frac{\Delta s}{U_x(s_k)} \sqrt{\left(\lambda\mu(s_k)g\right)^2 + \left(\kappa(s_k)U_x^2(s_k)\right)^2} \quad (16)$$

It starts from the maximum allowable vehicle speed at the end of the path and back toward to current station. At each step, the result is compared to the forward integral results. This step indicates how fast a vehicle can decelerate.

Fig. 6 shows the speed profile results for the example path.

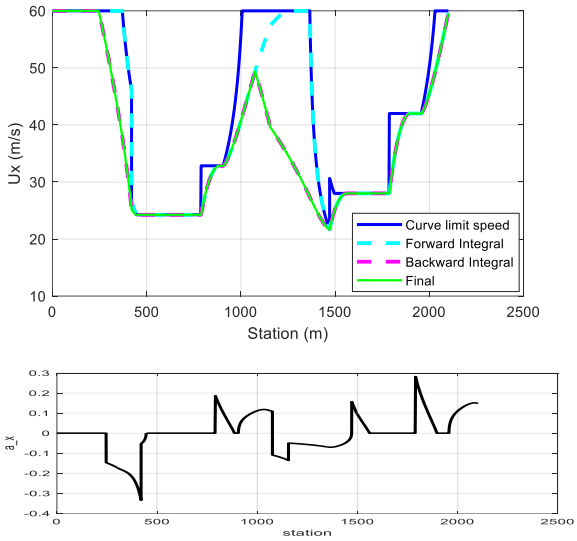

Figure 6. The intermediate and final results of the speed profile of the computation algorithm. We may not need to show ~~the acceleration~~

III. Preview Distance

In this section, we discuss the friction preview distance, which indicates how much friction data a vehicle needs to query from a database so that it can have sufficient time to take action for any upcoming situation.

Strategy can be: find the most critical scenario by case study.

A. Minimum Preview Distance given the Vehicle Current States

The criterion is that the vehicle has enough space to stop within the preview distance. The minimum curvature can be obtained from the path, and the minimum friction can be assumed to be 0.1 for conservation.

Case discussion: (the plot will be organized soon)

a. On the circle path, for a fixed initial speed, using the closed solution of (12) we can find the stop distance will be longer for lower friction and larger curvature. An interesting point is that the stop distance has an upper bound $4\pi/\kappa$. The reason is that the initial speed on the circular arc is limited by curvature and friction.
b. On the entering clothoid path, for a fixed initial speed, using the numerical solution of (12) we can find the stop distance will be longer for lower friction and larger curvature slope. And the stop distance is much large than case a with the same initial speed. The stop distance is approximately 350m for a 35m/s initial speed and friction coefficient of 0.2.
c. On line segment, the stop distance is shorter than entering the clothoid path.

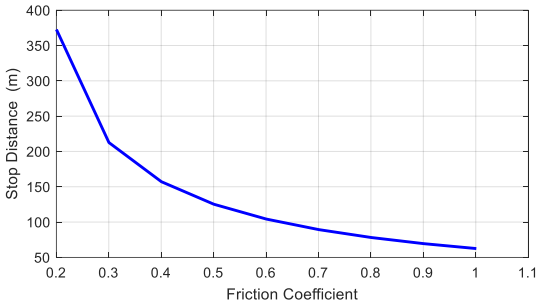

Figure 7. The stop distance on entering clothoid path with an initial spped of 35m/s and curvature slope 6.25×10^{-06}

[more plots]

The worst case is moving at the clothoid segment, ~~entering a circle,~~ with a sudden friction decrease.

Considering the delay of the driver, vehicle systems, and data transmission. The preview distance is a function of U_x, a_x, max(κ), assumed min μ, and constant.

$$d_{prev} = f(\kappa_{\max}, \mu_{\min}, U_x, a_x, c) \quad (17)$$

Most human drivers with the required driving vision can only see approximately XXXm even on a clear day when driving. Unfortunately, the visibility reduces a lot at adverse weather where dangerous road condition occurs.

And the driver's sight is limited at path corners and hills.

The friction preview is vital for safety.

B. Speed Profile Depends on the Preview Distance

The vehicle needs to move slower if with less visibility.

Both road condition and preview distance influence the vehicle speed profile.

IV. Application Case and Simulation Results

A vehicle with rear driving, front steering, understeering, or oversteering.

A path with a length of 5 km, compare the velocity results considering only curvature and the results considering both f friction and curvature.

A simple driver controller can follow the path well with the preview of friction.

A controller behavior with limited friction preview distance.

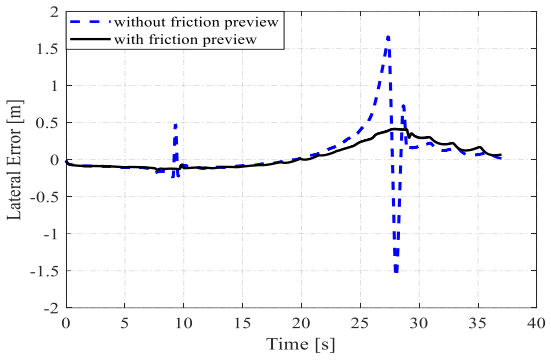

Figure 5. An apllication of preview

V. Conclusion

In this paper, we ... . The idea behind this is to extend individual intelligence with network intelligence.

Acknowledgment

This material is based upon work supported by the National Science Foundation under grant no. CNS-1932509 “CPS: Medium: Collaborative Research: Automated Discovery of Data Validity for Safety-Critical Feedback Control in a Population of Connected Vehicles”. And CNS-XXX, Dr. Beal and Dr. Jerath

References

[1] G. O. Young, “Synthetic structure of industrial plastics (Book style with paper title and editor),” in *Plastics*, 2nd ed. vol. 3, J. Peters, Ed. New York: McGraw-Hill, 1964, pp. 15–64.

[1] L. Yu, S. Zheng, Y. Dai, L. Abi, X. Liu, and S. Cheng, “A feedback-feedforward steering controller designed for vehicle lane keeping in hard-braking manoeuvres on split-μ roads,” *Veh. Syst. Dyn.*, 2021, doi: 10.1080/00423114.2020.1869274.

[2] L. Li, “PID PLUS FUZZY LOGIC METHOD FOR TORQUE CONTROL IN TRACTION CONTROL SYSTEM,” *Int. J. Automot. Technol.*, vol. 13, no. 3, pp. 441–450, 2012, doi: 10.1007/s12239.

[3] H. Cao, X. Song, S. Zhao, S. Bao, and Z. Huang, “An optimal model-based trajectory following architecture synthesising the lateral adaptive preview strategy and longitudinal velocity planning for highly automated vehicle,” *Veh. Syst. Dyn.*, vol. 55, no. 8, pp. 1143–1188, 2017, doi: 10.1080/00423114.2017.1305114.

[4] C. E. Beal and C. Boyd, “Coupled lateral-longitudinal vehicle dynamics and control design with three-dimensional state portraits,” *Veh. Syst. Dyn.*, vol. 57, no. 2, pp. 286–313, 2019, doi: 10.1080/00423114.2018.1467019.

[C. G. Bobier-Tiu, C. E. Beal, J. C. Kegelman, R. Y. Hindiyeh, and J. C. Gerdes, “Vehicle control synthesis using phase portraits of planar dynamics,” *Veh. Syst. Dyn.*, vol. 57, no. 9, pp. 1318–1337, 2019, doi: 10.1080/00423114.2018.1502456.

[S. Roychowdhury, M. Zhao, A. Wallin, N. Ohlsson, and M. Jonasson, “Machine Learning Models for Road Surface and Friction Estimation using Front-Camera Images,” in *2018 International Joint Conference on Neural Networks (IJCNN)*, 2018, pp. 1–8, doi: 10.1109/IJCNN.2018.8489188.

[C. E. Beal, “Rapid Road Friction Estimation using Independent Left/Right Steering Torque Measurements,” *Veh. Syst. Dyn.*, vol. 58, no. 3, pp. 377–403, 2020, doi: 10.1080/00423114.2019.1580377.

[J. Subosits and J. C. Gerdes, “Autonomous vehicle control for emergency maneuvers: The effect of topography,” *Proc. Am. Control Conf.*, vol. 2015-July, pp. 1405–1410, 2015, doi: 10.1109/ACC.2015.7170930.

[K. Kritayakirana and J. C. Gerdes, “Autonomous vehicle control at the limits of handling,” *Int. J. Veh. Auton. Syst.*, vol. 10, no. 4, pp. 271–296, 2012, doi: 10.1504/IJVAS.2012.051270.

[10] P. A. Theodosis and J. C. Gerdes, “Nonlinear optimization of a racing line for an autonomous racecar using professional driving techniques,” in *ASME 2012 5th Annual Dynamic Systems and Control Conference Joint with the JSME 2012 11th Motion and Vibration Conference, DSCC 2012-MOVIC 2012*, 2012, vol. 1, pp. 235–241, doi: 10.1115/DSCC2012-MOVIC2012-8620.

[11] N. R. Kapania, J. Subosits, and J. C. Gerdes, “A Sequential Two-Step Algorithm for Fast Generation of Vehicle Racing Trajectories,” *J. Dyn. Syst. Meas. Control. Trans. ASME*, vol. 138, no. 9, 2016, doi: 10.1115/1.4033311.

[12] W. C. Mitchell, R. Schroer, and D. B. Grisez, “Driving the traction circle,” *SAE Tech. Pap.*, no. 724, 2004, doi: 10.4271/2004-01-3545.

[13] C. E. Beal and J. C. Gerdes, “Model predictive control for vehicle stabilization at the limits of handling,” *IEEE Trans. Control Syst. Technol.*, vol. 21, no. 4, pp. 1258–1269, 2013, doi: 10.1109/TCST.2012.2200826.

[14] AASHTO, *A Policy on Geometric Design of Highways and Streets*. 2018.

[15] P. A. Theodosis and J. C. Gerdes, “Generating a racing line for an autonomous racecar using professional driving techniques,” *ASME 2011 Dyn. Syst. Control Conf. Bath/ASME Symp. Fluid Power Motion Control. DSCC 2011*, vol. 2, pp. 853–860, 2011, doi: 10.1115/DSCC2011-6097.

[16] J. Villagra, V. Milanés, J. Pérez, and J. Godoy, “Smooth path and speed planning for an automated public transport vehicle,” *Rob. Auton. Syst.*, vol. 60, pp. 252–265, 2012, doi: 10.1016/j.robot.2011.11.001.

[17] H. A. Hamersma and P. S. Els, “Longitudinal vehicle dynamics control for improved vehicle safety,” *J. Terramechanics*, vol. 54, pp. 19–36, 2014, doi: 10.1016/j.jterra.2014.04.002.

[18] R. Solea and U. Nunes, “Trajectory planning with velocity planner for fully-automated passenger vehicles,” *IEEE Conf. Intell. Transp. Syst. Proceedings, ITSC*, pp. 474–480, 2006, doi: 10.1109/itsc.2006.1706786.